Molecular Characterization and Expression Analysis of Annexin B3 and B38 as Secretory Proteins in *Echinococcus Granulosus*

Hongyu Song
Sichuan Agricultural University - Chengdu Campus
Xue He
Sichuan Agricultural University - Chengdu Campus
Xiaodi Du
Sichuan Agricultural University - Chengdu Campus
Ruiqi Hua
Sichuan Agricultural University - Chengdu Campus
Jing Xu
Sichuan Agricultural University - Chengdu Campus
Ran He
Sichuan Agricultural University - Chengdu Campus
Yue Xie
Sichuan Agricultural University - Chengdu Campus
Xiaobin Gu
Sichuan Agricultural University - Chengdu Campus
Xuerong Peng
Sichuan Agricultural University - Chengdu Campus
Guangyou Yang (guangyou1963@aliyun.com)
College of Veterinary Medicine, Sichuan Agricultural University

Research

Keywords: Echinococcus granulosus, Annexin, Calcium ion, Western blotting, Immunofluorescence localization, Secretory protein

Posted Date: November 24th, 2020

DOI: https://doi.org/10.21203/rs.3.rs-112153/v1

Version of Record: A version of this preprint was published at Parasites & Vectors on February 8th, 2021. See the published version at https://doi.org/10.1186/s13071-021-04596-7.

Abstract

Background: Cystic Echinococcosis is a parasitic zoonotic disease, which poses a threat to public health and animal husbandry, and causes significant economic losses. Annexin is a kind of phospholipid binding protein with calcium ion binding activity, which has many functions.

Methods: Two annexin protein family genes (*Eg*AnxB3 and *Eg*AnxB38) were cloned and molecular characterized using bioinformatic analysis. The immunoreactivity of r*Eg*AnxB3 and r*Eg*AnxB38 was investigated using western blotting. The distribution and transcript levels of *Eg*AnxB3 and *Eg*AnxB38 in different developmental stages of *Echinococcus granulosus* were analyzed by immunofluorescence localization and quantitative real-time reverse transcription PCR, and their secretory characteristics were analyzed preliminary. The phospholipid-binding activities of r*Eg*AnxB3 and r*Eg*AnxB38 were also tested.

Results: *Eg*AnxB3 and *Eg*AnxB38 are conserved and contain calcium binding sites. Both r*Eg*AnxB3 and r*Eg*AnxB38 could be specifically recognized by the serum samples from *E. granulosus*-infected sheep, which have strong immunoreactivity. *Eg*AnxB3 and *Eg*AnxB38 were distributed in all stages of *E. granulosus* and had high transcript levels in the 28-day strobilated worms. They were found in liver tissues near the cysts. In addition, r*Eg*AnxB3 had Ca^{2+}-dependent phospholipid-binding properties.

Conclusions: *Eg*AnxB3 and *Eg*AnxB38 contained calcium-binding sites, and r*Eg*AnxB3 had Ca^{2+}-dependent phospholipid-binding properties. r*Eg*AnxB3 and r*Eg*AnxB38 had strong immunoreactivity. *Eg*AnxB3 and *Eg*AnxB38 were transcribed in PSCs and worms. They were expressed in all stages of *E. granulosus*, and distributed in the liver tissues near the hydatid cyst, indicating that *Eg*AnxB3 and *Eg*AnxB38 are secreted proteins that play an crucial role in the development of *E. granulosus*.

Background

Cystic Echinococcosis (CE), caused by the larval stage of *Echinococcus granulosus*, is a parasitic zoonosis disease currently prevalent in Mediterranean countries, southern South America, Central Asia, Australia and parts of Africa [1, 2]. CE seriously threatens the development of public health and animal husbandry, causing about 3 billion US $ in economic losses each year [3]. It has been listed as one of the "Neglected Tropical Disease" by The World Health Organization (WHO) [4, 5].

Annexins are a kind of phospholipid binding proteins with calcium ion binding activity, which belong to the calcium signaling protein family and are widely distributed in eukaryotic cells [6]. According to the differences in gene location and protein structure, annexins are divided into five categories [7]. Annexins have multiple functions, such as cell anti-inflammatory, membrane repair, membrane transport, and probably participate in cell proliferation, differentiation, and apoptosis [8–12].

Parasite annexins have been known to regulate the host immune response and maintaining the structural integrity of the cell [13, 14]. Parasite annexins have also been considered as potential targets for the development of drug and vaccine candidates [13, 15]. *Leishmania* promastigotes could combine annexin

V to ensure normal function in the absence of phosphatidylserine [16]. Annexin 2 of *Schistosoma mansoni* is involved in epidermal development [17]. Recombinant annexin B30 of *S. mansoni* had no significant protection against the parasite, which suggested it may not be suitable as a vaccine candidate [18]. Annexin B1 of *Taenia solium* can downregulate the immune response of the host [19, 20]. Information concerning *E. granulosus* annexin is relatively scarce, and only *Eg*AnxB33 has been studied [21]. In the present study, cloning, expression, bioinformatic analysis, western blotting, relative fluorescence quantitative PCR, immunofluorescence localization, and phospholipidbinding bioactivity analysis of *Eg*AnxB3 and *Eg*AnxB38 were performed to provide basic information and new research directions for the interaction between *E. granulosus* and its hosts.

Materials And Methods

Animals

Four female New Zealand rabbits (9 weeks old) were purchased from Dashuo Experimental Animal Co., Ltd. (Chengdu, China, License Number of experimental animal Production: SYXK2019-189). Four male beagles (6 months old) were provided by Dujiangyan Beagle Breeding Center of Sichuan Institute of Musk Deer Breeding. Albendazole and levamisole were used for deworming in the first three months.

Parasites

Cysts of *E. granulosus* were seperated from naturally infected sheep in Sichuan Province, China. Protoscoleces (PSCs) and germinal layer were separated aseptically as described previously [22, 23]. The 28-day strobilated worms were acquired by artificially infected beagles. Each beagle was given 50 000 PSCs orally and euthanized after 28 days. The 18-day strobilated worms and 45-day adult worms were provided by the Department of Parasitology of Sichuan Agricultural University.

Sera

Sera against *E. granulosus* were isolated from naturally infected sheep. Negative sera were collected from cestode-free sheep. Corresponding sera were obtained in Sichuan Province, China and infection was determined by autopsy.

The preparation process of the polyclonal antibodies of r*Eg*AnxB3 and r*Eg*AnxB38 was the same as previously reported [23]. Briefly, rabbit sera were collected as a negative control before immunization. Then each rabbit was immunized with 200 μg recombinant protein emulsified with Freund's complete adjuvant (Sigma-Aldrich, St. Louis, MO, USA), followed by three boosters using Freund's incomplete adjuvant. Two weeks after the final immunization, antisera were isolated and immunoglobulin G (IgG) was extracted.

Cloning of *Eg*AnxB3 and *Eg*AnxB38

The RNA extraction kit (Tiangen, Beijing, China) was used to extract total RNA from PSCs, the Reverse Transcription System Kit (Takara, Dalian, China) was used to reverse transcribe into cDNA. Specific primers were designed at GenBank using the sequences of *Eg*AnxB3 and *Eg*AnxB38 (Accession numbers: XM_024495323.1 and XM_024494485.1, respectively). The sequence of *Eg*AnxB3 was amplified using the primers 5'-CGGATCCATGGCGACTGTCAAGCCTTGCTG -3' (*Bam*H I) and 5'-CCGGAATTCTTACTCCAGTATGGCAAGC -3' (*Eco*R I). The sequence encoding *Eg*AnxB38 was amplified using primers 5'- CGGATCCATGGCTGGCTATCCTCCACC -3' (*Bam*H I) and 5'-CGGAATTCTCAGGGTCCAACCAAAGCCAC -3' (*Eco*R I). Target fragments were amplified and cloned. Single colonies were selected for PCR identification, and the plasmid from the bacterial solution that tested positive by PCR was sequenced.

Bioinformatic analysis

The physicochemical properties were predicted using the Expasy proteomics server (http://au.expasy.org). The open reading frames (ORFs) of *Eg*AnxB3 and *Eg*AnxB38 were analyzed using ORF finder (https://www.ncbi.nlm.nih.gov/orffinder/). Signal peptides and transmembrane area were predicted using online software Signal IP (http://www.cbs.dtu.dk/services/SignalP-3.0/) and TMHMM-2.0 (http://www.cbs.dtu.dk/services/TMHMM-2.0/). Tertiary (3D) structures were modeled through SWISS-MODEL (http://swissmodel.expasy.org/). The MEGA software (version 5.05) was used to construct the phylogenetic tree using the maximum likelihood method (ML) [24].

Expression and Purification of Recombinant *Eg*AnxB3 and *Eg*AnxB38

The correctly sequenced *Eg*AnxB3 and *Eg*AnxB38 plasmids were digested with restriction enzymes, ligated into the pET32a (+) plasmid. The resulting recombinant plasmids were transformed into *Escherichia coli* BL21 (DE3) (Tiangen, Beijing, China). *E. coli* cells containing pET32a-*Eg*AnxB3 and pET32a-*Eg*AnxB38 were cultivated at 37 ℃ for 8 h. Then the transformants were induced with 1 mM isopropyl β-d-1-thiogalactopyranoside (IPTG). The recombinat proteins were purified using a Ni^{2+} affinity chromatography column (Bio-Rad, Hercules, CA, USA).

Western Blotting

Western blotting was performed as described previously [25]. Briefly, the crude protein extracts of PSCs and the purified recombinant protein were transferred onto a polyvinylidene difluoride membrane. The membrane was incubated with sera (1:200 v/v dilution) from infected sheep/goats or polyclonal antibodies (1:200 v/v dilution) for 12 h at 4 ℃. After four washes, horseradish peroxidase (HRP)-

conjugated sheep anti-rabbit IgG or rabbit anti-sheep/goat IgG (1:2000 v/v dilution, Boster, Wuhan, China) was added and incubated for 1 h at 37 ℃ . The immunoreactive protein signals were visualized using an Enhanced HRP-DAB Chromogenic Substrate Kit (Tiangen).

Quantitative Real-Time PCR

Total RNA and cDNA of PSCs and 28-day strobilated worms were obtained as described above. Quantitative real-time PCR was used to analyze expression profiles of *EgAnxB3* and *EgAnxB38* in PSCs and 28-day strobilated worms. The primers for *Eg*AnxB3 were 5'- TGCCAACACGGATGCCCAAAC -3' and 5'-CTGGTGCGGTGTGCGAGAAC -3'. The primers for *Eg*AnxB38 were 5'-CGCTACGCAGAGGACAAGAACG-3' and 5'-CTCGCATCTACCCAGCACCAAC-3'. Expression of the actin gene was detected for use as an internal control for normalization. Primers specific to *Eg*Actin were 5'- ATGGTTGGTATGGGACAAAAGG -3' and 5'-TTCGTCACAATACCGTGCTC -3'. The data were analyzed using the $2^{-\Delta\Delta CT}$ method [26].

Immunolocalization

The sections (PSCs, germinal layer from fertile/infertile cysts, 18-day strobilated worms and 45-day adult worms) were incubated with purified anti-r*Eg*AnxB3/anti-r*Eg*AnxB38 rabbit IgG or negative rabbit sera (1:200 v/v dilutions) for about 14 h at 4 ℃. Fluorescein isothiocyanate (FITC)-conjugated sheep anti-rabbit IgG (1:100 dilution in 0.1% Evans blue solution) was incubated with sections for 1 h at 37 ℃ in the dark. The fluorescence signals were observed under a fluorescence microscope. Meanwhile, to detect the possible secretion of *Eg*AnxB3 and *Eg*AnxB38, the liver tissues away from the cysts and near the cysts wall were also evaluated.

Phospholipid-binding bioactivity assay

The preparation of liposomes was based on previous reports with some modifications[21, 27]. Soybean Lecithin (0.9 g; Sangon, Shanghai, China) and 0.3 g of cholesterol (Sangon) were mixed and dissolved in Anhydrous ethanol in a small beaker, placed in a 65~70 ℃ water bath with stirring so that they dissolve completely, after which, the small beaker was rotated to remove the ethanol. 30 ml of preheated phosphate-buffered saline (PBS) was added to the beaker containing lecithin and cholesterol lipid membrane, and then stirred and hydrated in a water bath at 65 ~ 70℃ for 10 min. Finally, the small beaker was placed on the magnetic stirrer and stirred for 30 ~ 60 min. The phospholipid-binding assay was performed as described previously [21, 28]. Each recombinant protein had three experimental groups: A, B, and C. All groups were added with 20 μL liposomes, 30 μL *Eg*AnxB3/*Eg*AnxB38, 30 μL 1 mM $CaCl_2$ (except group C) and supplemented with 50 mM Tris-HCl to a total volume of 100 μL. All groups were incubated in ice water and centrifuged to separate the supernatant and precipitate. The precipitate in group B was washed with Tris-HCl. 30 μL of 1 mM EDTA and 70 μL of Tris-HCl were added to the precipitate of group B and incubated in ice water for 30 min. The supernatant and precipitate were

separated by centrifugation. All the supernatant and precipitate samples were analyzed using 12 % sodium dodecyl sulphate-polyacrylamide gel electrophoresis (SDS-PAGE).

Results

Gene amplification and bioinformatics analysis

The full length *Eg*AnxB3 sequence comprised 933 nucleotides and encoded a putative protein of 310 amino acids, with a theoretical molecular weight of about 34.8 kDa. The predicted isoelectric points (pI), lipid solubility coefficient, and instability coefficient of *Eg*AnxB3 were 5.37, 82.55, and 33.45, respectively. *Eg*AnxB38 contained ORF of 1 356 bp, encoding a putative protein of 451 amino acids, with a theoretical molecular weight of about 48.5 kDa. The predicted pI, lipid solubility coefficient, and instability coefficient of *Eg*AnxB38 were 6.66, 68.63, and 35.46, respectively. Both *Eg*AnxB3 and *Eg*AnxB38 were predicted to be extracellular proteins, but without a signal peptide.

Homology modeling was carried out on *Eg*AnxB3 and *Eg*AnxB38 in the swiss-Model database, and two proteins with high homology were found, whose PDB data numbers were 1ala.1.a and 1ail.1.a. Using them as templates, 3D models of *Eg*AnxB3 and *Eg*AnxB38 were constructed, respectively. The similarity between *Eg*AnxB3 and the template sequence was 45.75%, while the similarity was 39.31% between *Eg*AnxB38 and the template sequence. Both *Eg*AnxB3 and *Eg*AnxB38 have calcium binding sites. The difference is that *Eg*AnxB3 contains two types of calcium ion binding domain, while *Eg*AnxB38 only contains one calcium binding domain (Fig. 1).

DNAMAN was used to compare the protein sequences of *Eg*AnxB3 and *Eg*AnxB38, and it was found that the similarity was 32.15%. Multiple sequence alignment revealed that *Eg*AnxB3 shared 97.42% identity with *Echinococcus multilocularis* annexin, 83.23% with *Taenia solium* AnxB3, and 63.87% with *Hymenolepis microstoma* annexin. (Fig. 2 – 1). *Eg*AnxB38 shared 92.63% identity with *E. multilocularis* annexin, 64.13% with *H. microstoma* annexin, 40.17% with *Fasciola hepatica* annexin, and 39.88% with *Clonorchis sinensis* annexin (Fig. 2). The ML phylogenetic tree demonstrated *Eg*AnxB3 and *Eg*AnxB38 were located on different branches, and had the closest genetic relationship with *E. multilocularis* (Fig. 3).

Expression, Purification, and Western Blotting of r*Eg*AnxB3 and r*Eg*AnxB38

The molecular mass of *Eg*AnxB3 was about 52 kDa, which was close to the expected value (note: the pET-32a (+) His-tag weighs about 18 kDa). Solubility analysis showed that *Eg*AnxB3 was largely expressed as soluble form and partly in inclusion bodies (Fig. 4 – 1). The molecular mass of *Eg*AnxB38 was about 67 kDa. Solubility analysis showed that *Eg*AnxB38 was largely expressed in inclusion bodies (Fig. 4 – 2). Western blotting showed that r*Eg*AnxB3 and r*Eg*AnxB38 reacted with anti-r*Eg*AnxB3 and anti-r*Eg*-AnxB38 rabbit sera, respectively, and with CE-positive sheep sera. Moreover, the native *Eg*AnxB3

protein and *Eg*AnxB38 protein in crude protein from PSCs were recognized using the rabbit antir*Eg*AnxB3 antibody and rabbit anti-r*Eg*AnxB38 antibody, respectively (Fig. 4 – 1 and Fig. 4 – 2).

Transcriptional Profiles of *Eg*AnxB3 and *Eg*AnxB38

EgAnxB3 and *EgAnxB38* genes were transcribed in both PSCs and 28-day strobilated worms, and the transcript levels of *EgAnxB3* and *EgAnxB38* in 28-day strobilated worms were both significantly higher ($P < 0.05$) than those in PSCs (Fig. 5).

Immunolocalization of *Eg*AnxB3 and *Eg*AnxB38

*Eg*AnxB3 and *Eg*AnxB38 were distributed in the germinal layer of fertile/infertile cysts, the parenchyma and tegument of 18-day strobilated and 45-day adult worms, and the calcareous corpuscles and hooks of PSCs. Compared with *Eg*AnxB3, *Eg*AnxB38 was not only distributed in the calcareous corpuscles and hooks of PSCs, but also distributed in the tegument of PSCs. Meanwhile, the distribution range of *Eg*AnxB38 in fertile/infertile cyst, adult worm, and PSC was significantly higher than that of *Eg*AnxB3, showing a strong fluorescence signal (Fig. 6).

*Eg*AnxB3 and *Eg*AnxB38 were distributed in hepatic sinusoids of liver tissue close to hydatid cysts. In addition, *Eg*AnxB38 was also found in hepatic sinusoids in the live distant from the hydatid cysts, whereas *Eg*AnxB3 was not found in this area (Fig. 7).

Phospholipid-binding bioactivity analysis.

Recombinant *Eg*AnxB3 and *Eg*AnxB38 were reacted with lipidosomes in the presence or absence of Ca^{2+} to examine their calcium-dependent phospholipid-binding properties. Mixtures were centrifuged, and the bound protein was pelleted with the precipitate and the unbound protein remained in the supernatant. In the presence of Ca^{2+}, r*Eg*AnxB3 was observed in the precipitate rather than supernatant (group A). When Ca^{2+} was removed from the recombinant protein using EDTA, r*Eg*AnxB3 largely remained in the supernatant (group B). r*Eg*AnxB3 was mainly observed in the supernatant in the absence of Ca^{2+} (group C). However, r*Eg*AnxB38 was observed in both the precipitate and supernatant, regardless of the presence of Ca^{2+} (Fig. 8).

Discussion

The classification and nomenclature of annexin B group is confusing. Generally, parasites are invertebrates, and annexin should be named as annexin B. However, when we screened these two genes at the NCBI based on the Zheng's research in 2013 [29], they were both called AnxA7, which is obviously inaccurate. We found that *Eg*AnxB3 had high similarity with *T. solium* annexin B3 via sequence

alignment, so we named it as *Eg*AnxB3. However, when naming *Eg*AnxB38, it was too hard to find a similar sequence from a parasite to compare it with and also name it accurately. Then, we found an article that named the annexins of many parasites by sequence alignment and phylogenetic tree analysis, including the naming of the annexin of *E. granulosus* [30]. We searched according to its website (http://www.structuralchemistry.org/annexins/seq/search.php), which showed that our naming of *Eg*AnxB3 is correct, and the naming of *Eg*AnxB33 is also consistent with the published article [21]. Therefore, we confirmed the naming of *Eg*AnxB38 instead of AnxA7 in this article.

Annexin proteins generally have four homologous repeat domains, and most of the domains contain a typical sequence of K-G-X-G-T. It has been reported that the calcium binding capacity is based on the K-G-X-G-T sequence [30–32]. Amino acid sequence analysis showed that both *Eg*AnxB3 and *Eg*AnxB38 had four repeat domains and contained a K-G-X-G-T sequence. The tertiary structures of *Eg*AnxB3 and *Eg*AnxB38 were predicted, both *Eg*AnxB3 and *Eg*AnxB38 were found to have Ca^{2+} binding sites. To verify the calcium binding ability of r*Eg*AnxB3 and r*Eg*AnxB38, we conducted a Ca^{2+}dependent phospholipid-binding assay and found that in the absence of Ca^{2+}, r*Eg*AnxB3 could not bind to liposomes and existed in the supernatant, while in the presence of Ca^{2+}, r*Eg*AnxB3 bound with liposomes and existed in the precipitate. When EDTA was added to combine with calcium ions, *Eg*AnxB3 returned to the supernatant, indicating that r*Eg*AnxB3 had Ca^{2+}-dependent phospholipid-binding properties. However, the Ca^{2+} dependent phospholipid binding properties of r*Eg*AnxB38 were relative weak. r*Eg*AnxB38 was observed in both the precipitate and supernatant, regardless of the presence of Ca^{2+}. There are two possible reasons. First, *Eg*AnxB38 was expressed in this study as an inclusion body protein, and thus possibly did not fold correctly, resulting in a lack of calcium binding capacity. Second, regardless of the amino acid structure analysis or tertiary structure prediction, *Eg*AnxB38 had fewer Ca^{2+} binding sites, resulting in an insufficient calcium binding capacity.

The transcript level of annexins vary at various stages of parasite development. *T. multiceps* AnxB2 and AnxB12 show high levels of transcription in the oncosphere. The transcript levels of *AnxB2* and *AnxB12* decreased from oncospheres to adults, while that of *AnxB3* increased [31]. The transcript level of *C. sinensis AnxB30* is higher in the metacercaria stage, and lower in adult worms and eggs [33]. The transcript levels of *EgAnxB3 a*nd *EgAnxB38* in the 28-day strobilated worm were higher than those of PSCs in this study, suggesting that *Eg*AnxB3 and *Eg*AnxB38 might have an crucial role in the process of PSCs invading the definitive host.

The parasite contacts with the host through the tegument, and the molecules distributed in the tegument participate in the host-parasite interaction, including excretion, nutrient absorption, and interaction with the host immune system [34, 35]. In the present study, *Eg*AnxB3 and *Eg*AnxB38 were found to be located in the tegument and parenchymatous tissue of immature and gravid proglottids, on the basis of immunofluorescence localization analysis, and *Eg*AnxB38 had a wider distribution and stronger fluorescence intensity, indicating that these two proteins might have an paramount role in the process of PSCs invasion of the definitive host and in self-development, with *Eg*AnxB38 possibly playing a larger

role in this process. Meanwhile, *Eg*AnxB38 was distributed in the hooks and tegument of PSCs, while *Eg*AnxB3 is not distributed or distributed at a much lower level in these two parts of PSCs. Considering that PSCs require the participation of the hook during the development of the definitive host's intestines, it is speculated that *Eg*AnxB38 participates in the interaction between the PSCs and the definitive host. PSCs form and mature in the germinal layer of *E. granulosus* [36]. *Eg*AnxB3 and *Eg*AnxB38 were distributed in the germinal layer, and their distribution range in fertile cysts was larger than in infertile cysts, suggesting that *Eg*AnxB3 and *Eg*AnxB38 might be related to the growth and development of PSCs.

Most annexins are cytoplasmic proteins or cytoskeletal proteins [37]; however, traces of annexins have also been found in the extracellular regions, although these annexins lack the signal peptide sequences required for extracellular secretion [38–40]. This interesting phenomenon suggested that some annexins are secreted. *C. sinensis* AnxB30 is a secretory protein that is involved in the interaction between the parasite and host, and affects the host's autoimmune response [33]. As a secreted protein, *T. solium* AnxB1 is involved in the interaction with the host inflammatory cells [13, 19, 20]. Annexin was also found to be present in the ES product and hydatid cyst fluid of *E. granulosus* [41, 42]. *Eg*AnxB33 was distributed in the interaction site of the liver tissue and hydatid cysts, suggesting that it might play an paramount role in the interaction between *E. granulosus* and the host [21]. Although *Eg*AnxB3 and *Eg*AnxB38 have no signal peptide, in this study, *Eg*AnxB3 and *Eg*AnxB38 was found to be located in the hepatic sinusoids of liver tissue near hydatid cysts. *Eg*AnxB38 was also found to be distributed in hepatic sinusoids in the liver, which was far away from the cysts. These observations indicated that they can be secreted into the extracellular areas to exert their physiological activities through nonclassical secretion pathways, such as transfer via extracellular vesicles. However, their specific function in the relationship between the host and the parasite need to be further investigated.

Conclusion

In conclusion, we found that both *Eg*AnxB3 and *Eg*AnxB38 contained calciumbinding sites, and r*Eg*AnxB3 had Ca^{2+} dependent phospholipid-binding properties. Both r*Eg*AnxB3 and r*Eg*AnxB38 could be specifically recognized by CE-positive sheep sera, indicating that they had strong immunoreactivity. The transcription level of *Eg*AnxB3 and *Eg*AnxB38 in 28-day strobilated worms was higher than that in PSCs *Eg*AnxB3 and *Eg*AnxB38 were distributed in all stages of *E. granulosus*, and were also distributed in the liver tissues near hydatid cysts, indicating that *Eg*AnxB3 and *Eg*AnxB38 are secreted proteins that might play an crucial role in the development of *E. granulosus*.

Abbreviations

r*Eg*AnxB3: recombinant *E. granulosus* annexin B3; r*Eg*AnxB38: recombinant *E. granulosus* annexin B38; PSCs: protoscoleces; PBS: phosphate-buffered saline; ORF: the open reading frame; IPTG: isopropyl β-d-1-thiogalactopyranoside; SDS-PAGE: sodium dodecyl sulphate-polyacrylamide gel electrophoresis; HRP: horseradish peroxidase; BSA: bovine serum albumin; PCR: polymerase chain reaction; FITC: fluorescein isothiocyanate; IgG: immunoglobulin G; EDTA: Ethylene Diamine Tetraacetic Acid.

Declarations

Acknowledgements

The authors thank Jie Xiao, Yuejun Luo, and Song Liu (Sichuan Agricultural University) for their help in performing the experiments. We also thank Lang Xiong, Ke Guan, Jiafei Zhan, and Nengxing Shen (Sichuan Agricultural University) for their constructive suggestions on the manuscript preparation. We would like to thank the native English speaking scientists of Elixigen Company (Huntington Beach, California) for editing our manuscript.

Ethics approval and consent to participate

The animal study was reviewed and approved by the Animal Care and Use Committee of Sichuan Agricultural University (SYXK2019-187). All animal procedures used in this study were carried out in accordance with the Guide for the Care and Use of Laboratory Animals (National Research Council, Bethesda, MD, USA) and recommendations of the ARRIVE guidelines (https://www.nc3rs.org.uk/arrive-guidelines). All methods were carried out in accordance with relevant guidelines and regulations.

Consent for publication

Not applicable.

Availability of data and materials

The datasets supporting the conclusions of this article are included within the article.

Competing interests

The authors declare that they have no conflict of interest.

Funding

This research was funded by the National Natural Science Foundation of China (Grant No. 31672547) and the Key TechnologyR&D Program of Sichuan Province, China (No. 2020YFN0030)

Authors' contributions

SHY participated in the design of the study, feeding experimental animals, the experiments, statistical analysis and manuscript writing. HX and DXD performed the experiments. HRQ contributed to sample collection and performed the experiments. XJ, HR and YGY participated in the design of the study. GXB, XY and PXR helped in study design. All authors read and approved the final manuscript.

References

1. Deplazes P, Rinaldi L, Rojas CAA, Torgerson PR, Jenkins EJ. Global distribution of alveolar and cystic echinococcosis. Adv Parasit. 2017;95:315-493.
2. Othieno E, Ocaido M, Mupere E, Omadang L, Oba P, Okwi AL. Knowledge, attitude, and beliefs of communities and health staff about *Echinococcus granulosus* infection in selected pastoral and agropastoral regions of Uganda. J Parasitol Res. 2018;2018:1-10.
3. Rialch A, Raina OK, Tigga MN, Anandanarayanan A, Verma MR. Evaluation of *Echinococcus granulosus* recombinant *Eg*AgB8/1, *Eg*AgB8/2 and EPC1 antigens in the diagnosis of cystic echinococcosis in buffaloes. Vet Parasitol. 2018;252:29-34.
4. Organization WH. Investing to overcome the global impact of neglected tropical diseases: third WHO report on neglected tropical diseases 2015. vol. 3: World Health Organization; 2015.
5. Wen H, Vuitton L, Tuxun T, Li J, Vuitton DA, Zhang W, et al. Echinococcosis: advances in the 21st century. Clin Microbiol Rev. 2019;32:1-39.
6. Schloer S, Pajonczyk D, Rescher U. Annexins in translational research: hidden treasures to be found. Int J Mol Sci. 2018;19:1781.
7. Gerke V, Creutz CE, Moss SE. Annexins: linking Ca^{2+} signalling to membrane dynamics. Nat Rev Mol Cell Bio. 2005;6:449-61.
8. Chander A, Chen XL, Naidu DG. A role for diacylglycerol in annexin A7-mediated fusion of lung lamellar bodies. BBA-Mol Cell Biol L. 2007;1771:1308-18.
9. Mortimer JC, Laohavisit A, Macpherson N, Webb AAR, Brownlee C, Battey NH, et al. Annexins: multifunctional components of growth and adaptation. J Exp Bot. 2008;59:533-44.
10. Rescher U, Gerke V. Annexins - unique membrane binding proteins with diverse functions. J Cell Sci. 2004;117:2631-9.
11. Monastyrskaya K. Functional association between regulatory RNAs and the annexins. Int J Mol Sci. 2018;19:591.
12. Boye TL, Nylandsted J. Annexins in plasma membrane repair. Biol Chem. 2016;397:961-9.
13. Hofmann A, Osman A, Leow CY, Driguez P, Mcmanus DP, Jones MK. Parasite annexins-new molecules with potential for drug and vaccine development. Bioessays. 2010;32:967-76.
14. Lu Y, Wang N, Wang J, Wang K, Sun S. Expression, purification, and characterization of a novel Ca^{2+}- and phospholipid-binding protein annexin B2. Mol Biol Rep. 2010;37:1591-6.
15. Jenikova G, Hruz P, Andersson MK, Tejman-Yarden N, Ferreira PC, Andersen YS, et al. α1-giardin based live heterologous vaccine protects against *Giardia* lamblia infection in a murine model. Vaccine. 2011;29:9529-37.
16. Weingärtner A, Kemmer G, Müller FD, Zampieri RA, dos Santos MG, Schiller J, et al. *Leishmania* promastigotes lack phosphatidylserine but bind annexin V upon permeabilization or miltefosine treatment. PloS one. 2012;7:e42070.
17. Tararam CA, Farias LP, Wilson RA, Leite LCC. *Schistosoma mansoni* annexin 2: molecular characterization and immunolocalization. Exp Parasitol. 2010;126:146-55.

18. Leow CY, Willis C, Chuah C, Leow CH, Jones M. Immunogenicity, antibody responses and vaccine efficacy of recombinant annexin B30 against *Schistosoma mansoni*. Parasite Immunol. 2020;42:e12693.
19. Gao Y, Yan H, Ding F, Lu Y, Sun S. Annexin B1 at the host–parasite interface of the *Taenia solium* cysticercus: secreted and associated with inflammatory reaction. Acta Trop. 2007;101:192-9.
20. Yan H, Xue G, Mei Q, Ding F, Wang Y, Sun S. Calcium-dependent proapoptotic effect of *Taenia solium* metacestodes annexin B1 on human eosinophils: A novel strategy to prevent host immune response. Int J Biochem Cell Biol. 2008;40:2151-63.
21. Song X, Hu D, Zhong X, Wang N, Gu X, Wang T, et al. Characterization of a secretory annexin in *Echinococcus granulosus*. Am J Trop Med Hyg. 2016;94:626-33.
22. Khan A, El-Buni A, Ali M. Fertility of the cysts of *Echinococcus granulosus* in domestic herbivores from Benghazi, Libya, and the reactivity of antigens produced from them. Ann Trop Med Parasitol. 2001;95:337-42.
23. Zhan J, Song H, Wang N, Guo C, Shen N, Hua R, et al. Molecular and functional characterization of inhibitor of apoptosis proteins (IAP, BIRP) in *Echinococcus granulosus*. Front Microbiol. 2020;11:729.
24. Tamura K, Peterson D, Peterson N, Stecher G, Nei M, Kumar S. MEGA5: molecular evolutionary genetics analysis using maximum likelihood, evolutionary distance, and maximum parsimony methods. Mol Biol Evol. 2011;28:2731-9.
25. Xu J, Huang X, He M, Ren Y, Shen N, Li C, et al. Identification of a novel PYP-1 gene in *Sarcoptes scabiei* and its potential as a serodiagnostic candidate by indirect-ELISA. Parasitology. 2018;145:752-61.
26. Livak KJ, Schmittgen TD. Analysis of relative gene expression data using real-time quantitative PCR and the $2^{-\Delta\Delta CT}$ method. Methods. 2001;25:402-8.
27. Zhang Y, Wang K, Guo Y, Lu Y, Yan H, Song Y, et al. Annexin B1 from *Taenia solium* metacestodes is a newly characterized member of the annexin family. Biol Chem. 2007;388:601-10.
28. Choi S, Kwon S, Lee E, Kim K. Molecular cloning, functional characterization and localization of an annexin from a fish gill fluke Microcotyle sebastis (Platyhelminthes: Monogenea). Mol Biochem Parasitol. 2009;163:48-53.
29. Zheng H, Zhang W, Zhang L, Zhang Z, Li J, Lu G, et al. The genome of the hydatid tapeworm *Echinococcus granulosus*. Nat Genet. 2013;45:1168-75.
30. Cantacessi C, Seddon JM, Miller TL, Leow CY, Thomas L, Mason L, et al. A genome-wide analysis of annexins from parasitic organisms and their vectors. Sci Rep. 2013;3:1-8.
31. Guo C, Xie Y, Liu Y, Wang N, Zhan J, Zhou X, et al. Molecular characterization of annexin B2, B3 and B12 in *Taenia multiceps*. Genes. 2018;9:559.
32. Morgan R, Martin-Almedina S, Iglesias J, Gonzalez-Florez M, Fernandez M. Evolutionary perspective on annexin calcium-binding domains. BBA-Mol Cell Res. 2004;1742:133-40.

33. He L, Ren M, Chen X, Wang X, Li S, Lin J, et al. Biochemical and immunological characterization of annexin B30 from *Clonorchis sinensis* excretory/secretory products. Parasitol Res. 2014;113:2743-55.
34. Simpson AJG, Smithers SR. Schistosomes: surface, egg and circulating antigens. Curr Top Microbiol Immunol. 1985;120:205-39.
35. Dalton JP, Skelly PJ, Halton DW. Role of the tegument and gut in nutrient uptake by parasitic platyhelminths. Can J Zool. 2004;82:211-32.
36. Galindo M, Schadebrodt G, Galanti N. *Echinococcus granulosus*: cellular territories and morphological regions in mature protoscoleces. Exp Parasitol. 2008;119:524-33.
37. Gerke V, Moss SE. Annexins : from structure to function. Physiol Rev. 2002;82:331-71.
38. Vergnolle N, Pages P, Guimbaud R, Chaussade S, Bueno L, Escourrou J, et al. Annexin 1 is secreted in situ during ulcerative colitis in humans. Inflamm Bowel Dis. 2004;10:584-92.
39. Donnelly SR, Moss SE. Annexins in the secretory pathway. Cell Mol Life Sci. 1997;53:533-8.
40. Samia Y, Ajantha S, Egle S, Virginia C, Flower RJ, Bernhard R. Anti-allergic cromones inhibit histamine and eicosanoid release from activated human and murine mast cells by releasing Annexin A1. Plos One. 2013;8:e58963.
41. Virginio VG, Monteiro KM, Drumond F, de Carvalho MO, Vargas DM, Zaha A, et al. Excretory/secretory products from in vitro-cultured *Echinococcus granulosus* protoscoleces. Mol Biochem Parasitol. 2012;183:15-22.
42. Aziz A, Zhang W, Li J, Loukas A, McManus DP, Mulvenna J. Proteomic characterisation of *Echinococcus granulosus* hydatid cyst fluid from sheep, cattle and humans. J Proteomics. 2011;74:1560-72.

Figures

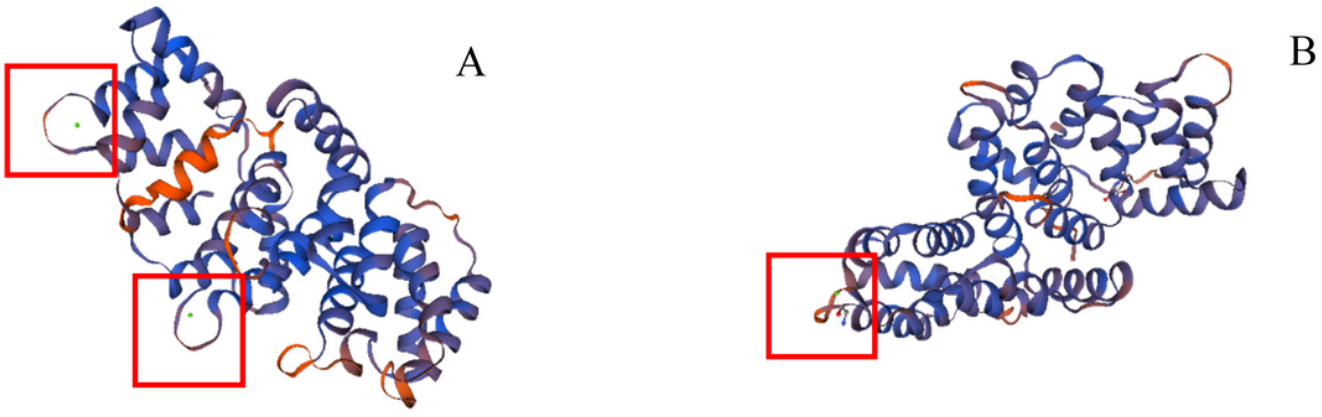

Figure 1

3D structure model prediction of EgAnxB3 and EgAnxB38. A: EgAnxB3; B: EgAnxB38, the red box area shows the calcium ion binding area.

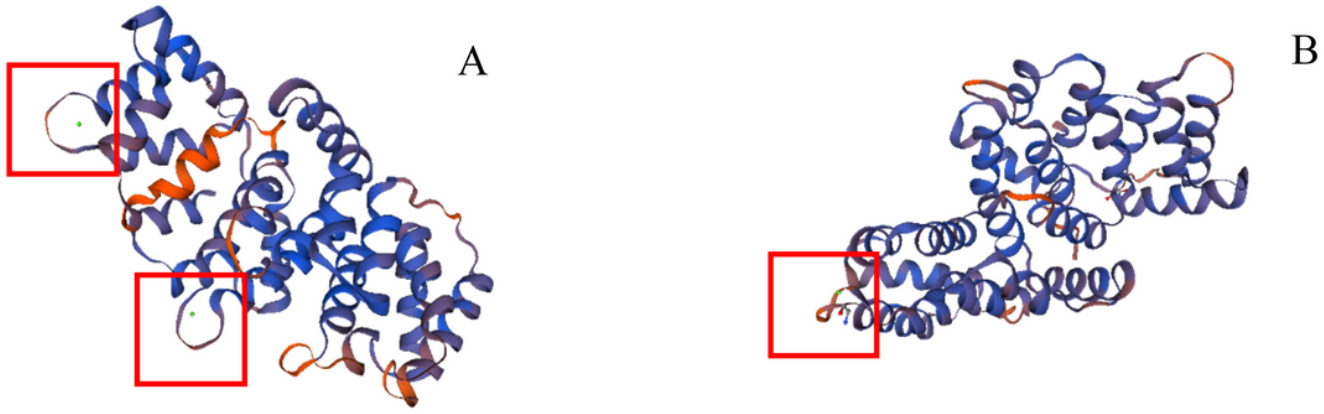

Figure 1

3D structure model prediction of EgAnxB3 and EgAnxB38. A: EgAnxB3; B: EgAnxB38, the red box area shows the calcium ion binding area.

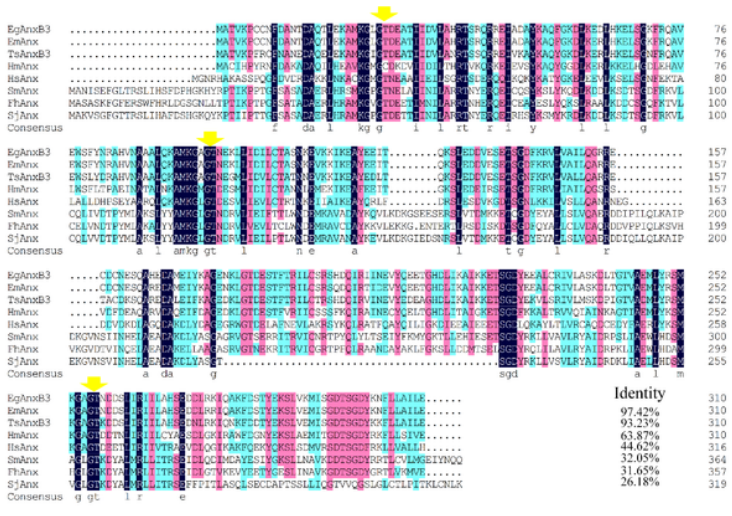

2-1

2-2

Figure 2

2-1 Sequence alignment of EgAnxB3. Note: K-G-X-G-T sequence represented by yellow arrows. Eg: Echinococcus granulosus (gb: XP_024350278.1); Em: Echinococcus multilocularis (gb: CDI98572.1); Ts: Taenia solium (gb: AAY27744.1); Hm: Hymenolepis microstoma (gb: CDS27549.1); Hs: Homo sapiens (gb: CAG46637.1); Sm: Schistosoma mansoni (gb: AAC79802.3); Fh：Fasciola hepatica (gb: THD28189.1); Sj : Schistosoma japonicum (gb: TNN13360.1). 2-2 Sequence alignment of EgAnxB38. Note: K-G-X-G-T sequence represented by yellow arrows. Eg: Echinococcus granulosus (gb: CDS24484.1);

Em: Echinococcus multilocularis (gb: CDS35601.1); Hm: Hymenolepis microstoma (gb: CDS26802.2); Fh Fasciola hepatica (gb: THD25992.1); Cs: Clonorchis sinensis (gb: RJW68544.1); Ov: Opisthorchis viverrini (gb: OON18674.1); Sh: Schistosoma haematobium (gb: XP_012796077.1); Hs: Homo sapiens (gb: AAH00871.1).

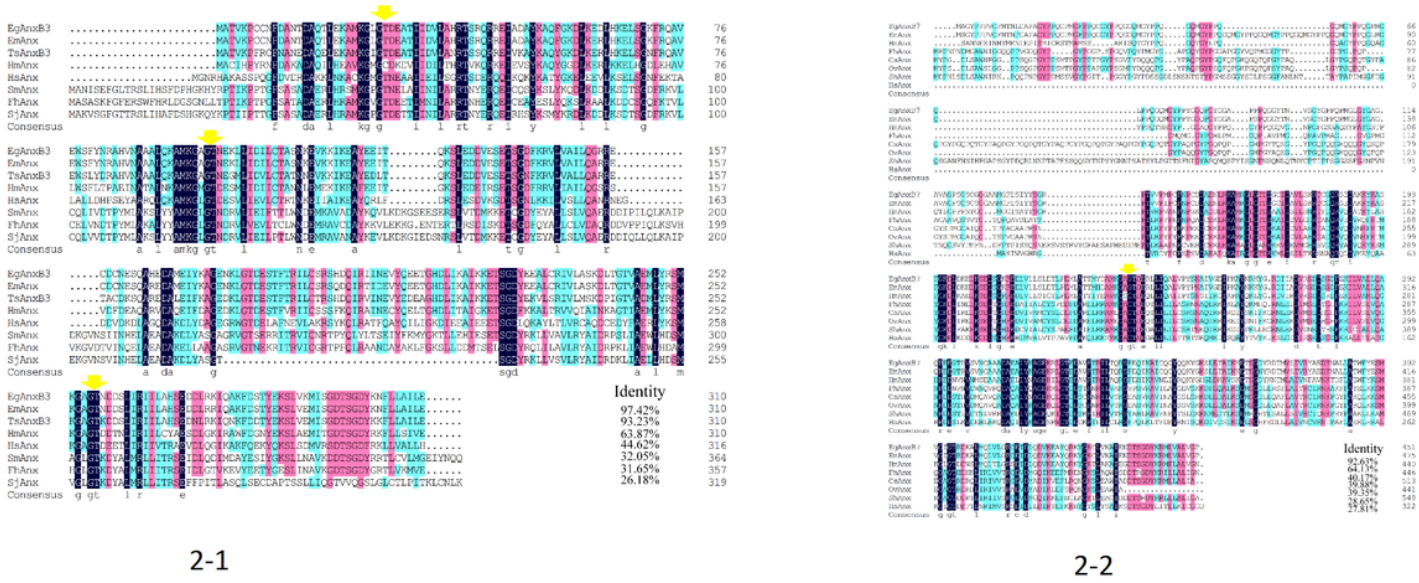

2-1 2-2

Figure 2

2-1 Sequence alignment of EgAnxB3. Note: K-G-X-G-T sequence represented by yellow arrows. Eg: Echinococcus granulosus (gb: XP_024350278.1); Em: Echinococcus multilocularis (gb: CDI98572.1); Ts: Taenia solium (gb: AAY27744.1); Hm: Hymenolepis microstoma (gb: CDS27549.1); Hs: Homo sapiens (gb: CAG46637.1); Sm: Schistosoma mansoni (gb: AAC79802.3); Fh Fasciola hepatica (gb: THD28189.1); Sj : Schistosoma japonicum (gb: TNN13360.1). 2-2 Sequence alignment of EgAnxB38. Note: K-G-X-G-T sequence represented by yellow arrows. Eg: Echinococcus granulosus (gb: CDS24484.1); Em: Echinococcus multilocularis (gb: CDS35601.1); Hm: Hymenolepis microstoma (gb: CDS26802.2); Fh Fasciola hepatica (gb: THD25992.1); Cs: Clonorchis sinensis (gb: RJW68544.1); Ov: Opisthorchis viverrini (gb: OON18674.1); Sh: Schistosoma haematobium (gb: XP_012796077.1); Hs: Homo sapiens (gb: AAH00871.1).

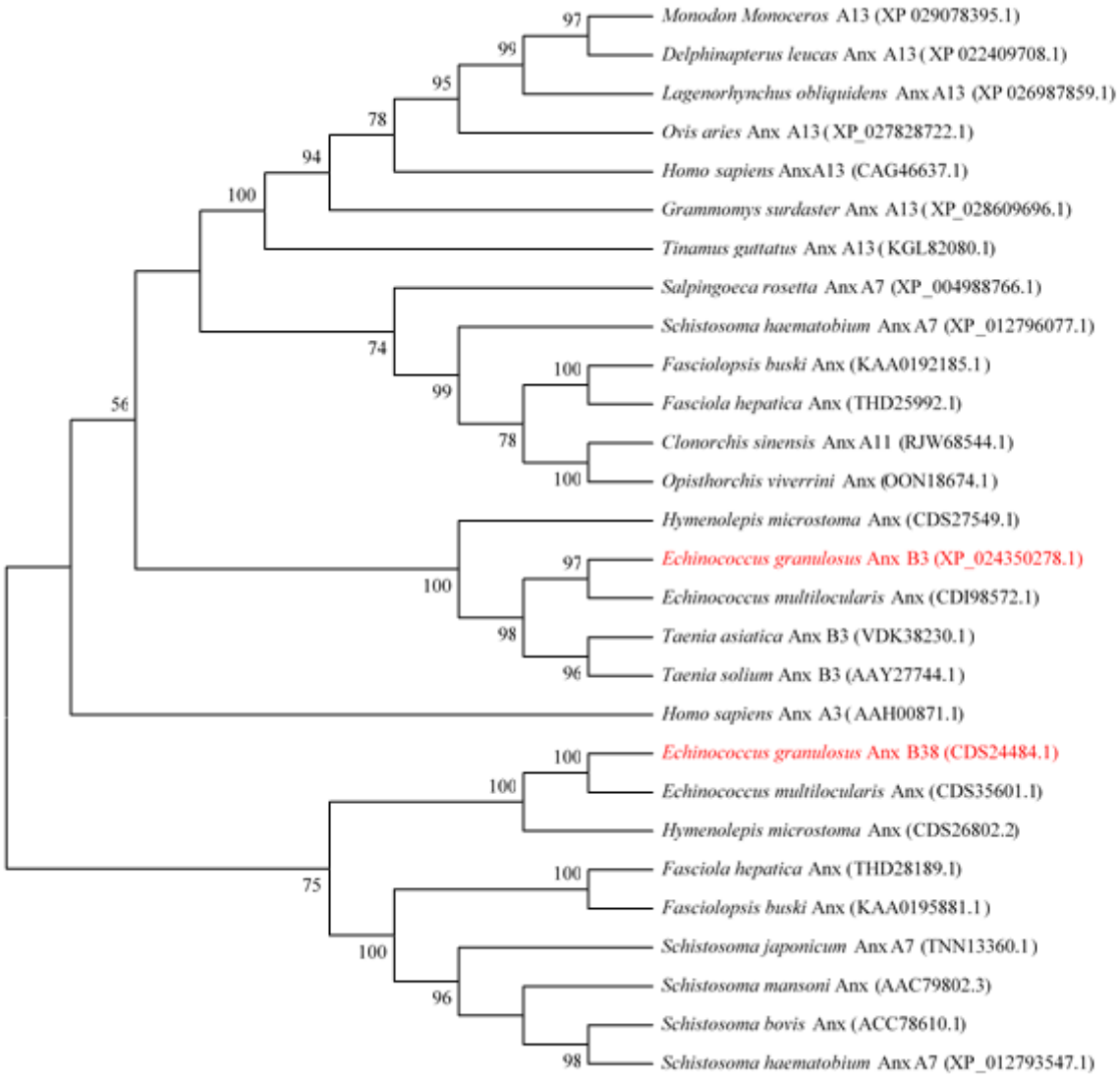

Figure 3

The ML phylogenetic tree of EgAnxB3 and EgAnxB38.

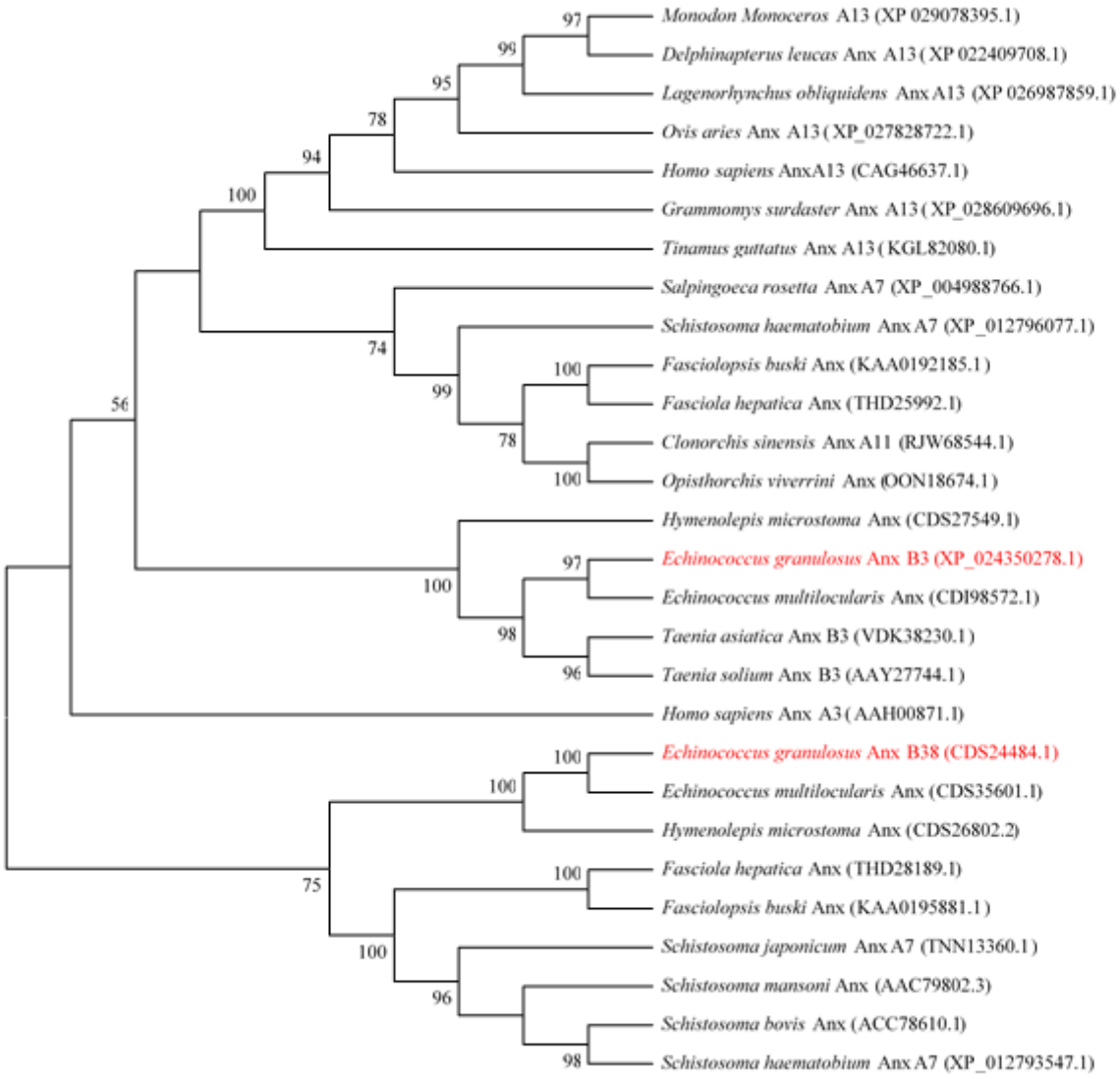

Figure 3

The ML phylogenetic tree of EgAnxB3 and EgAnxB38.

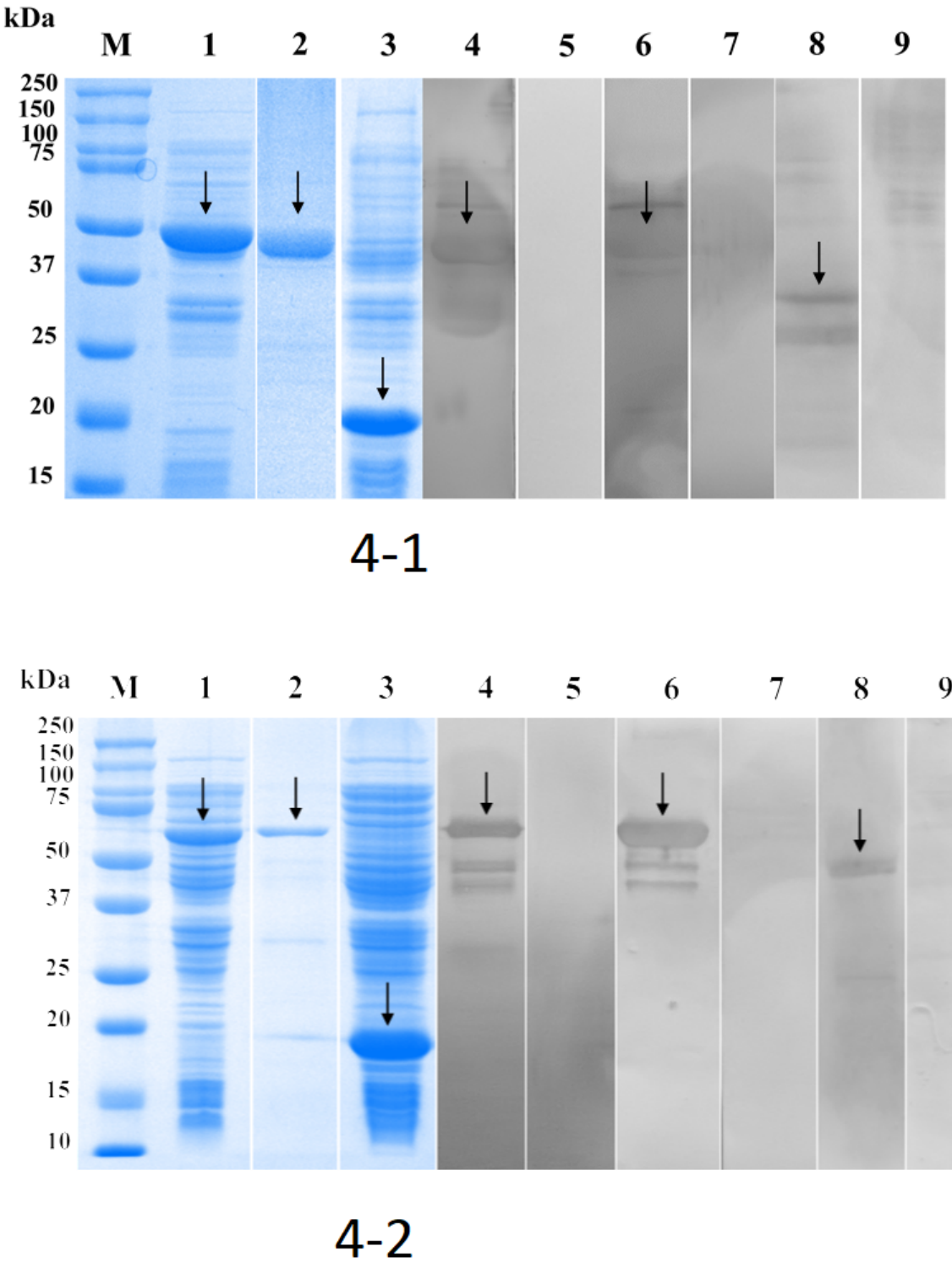

Figure 4

4-1 Purification and western blotting of EgAnxB3. M: Protein marker; 1. rEgAnxB3 crude protein; 2. Purified rEgAnxB3; 3. pET32a(+) induced by IPTG; 4. rEgAnxB3 incubated with rabbit anti-rEgAnxB3-IgG; 5. rEgAnxB3 incubated with negative rabbit serum IgG; 6. rEgAnxB3 incubated with sera from a sheep infected with E. granulosus; 7. rEgAnxB3 incubated with serum of healthy sheep; 8: Crude protein of PSCs incubated with rabbit anti-rEgAnxB3-IgG; 9: Crude protein of PSCs incubated with negative rabbit serum

IgG. 4-2 Purification and western blotting of EgAnxB38. M: Protein marker; 1. EgAnxB38 crude protein; 2. Purified EgAnxB38; 3.pET32a (+) induced by IPTG; 4. EgAnxB38 incubated with rabbit anti-EgAnxB38-IgG; 5. EgAnxB38 incubated with negative rabbit serum IgG; 6. EgAnxB38 incubated with sera from a sheep infected with E. granulosus; 7. EgAnxB38 incubated with serum of healthy sheep; 8. Crude protein of PSCs incubated with rabbit anti-EgAnxB38-IgG; 9. Crude protein of PSCs incubated with negative rabbit serum IgG.

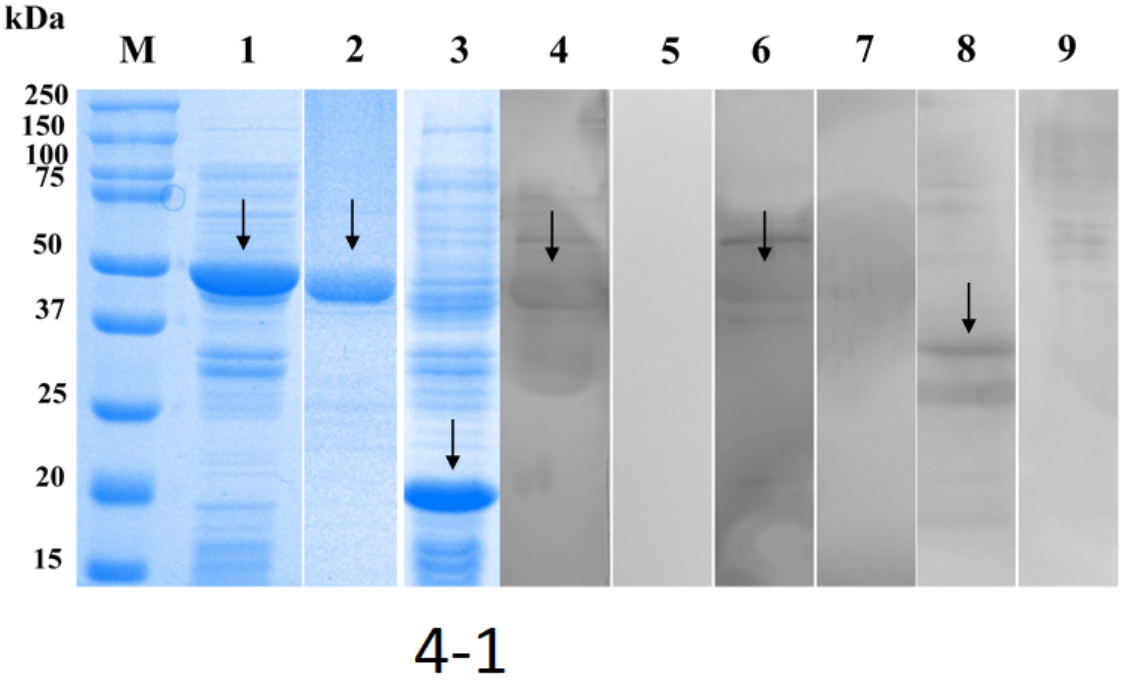

4-1

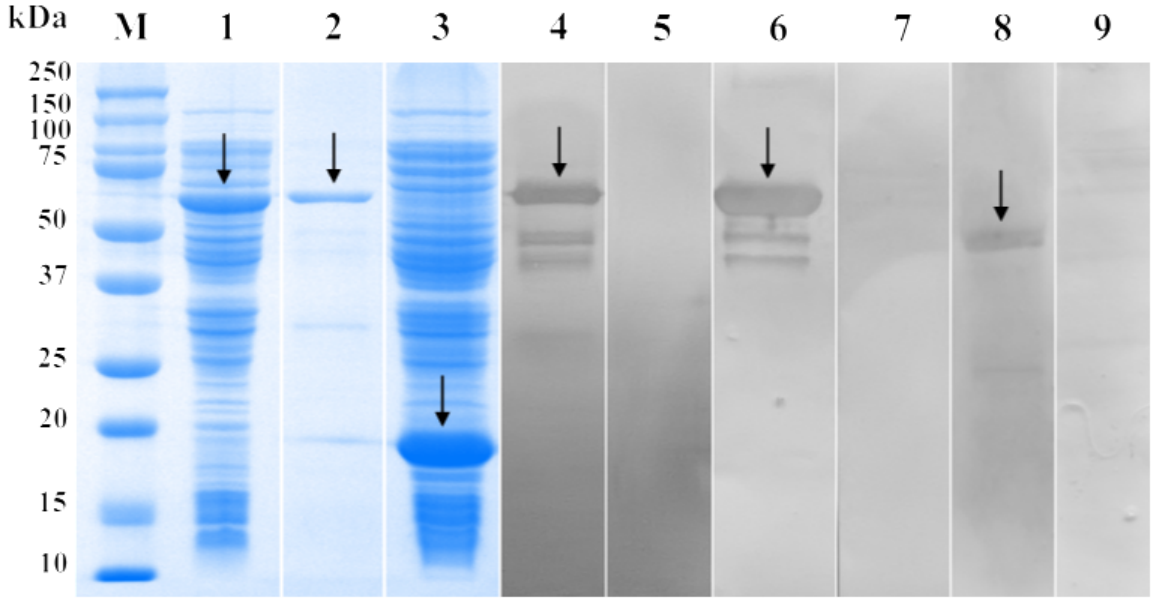

4-2

Figure 4

4-1 Purification and western blotting of EgAnxB3. M: Protein marker; 1. rEgAnxB3 crude protein; 2. Purified rEgAnxB3; 3. pET32a(+) induced by IPTG; 4. rEgAnxB3 incubated with rabbit anti-rEgAnxB3-IgG; 5. rEgAnxB3 incubated with negative rabbit serum IgG; 6. rEgAnxB3 incubated with sera from a sheep infected with E. granulosus; 7. rEgAnxB3 incubated with serum of healthy sheep; 8: Crude protein of PSCs incubated with rabbit anti-rEgAnxB3-IgG; 9: Crude protein of PSCs incubated with negative rabbit serum IgG. 4-2 Purification and western blotting of EgAnxB38. M: Protein marker; 1. EgAnxB38 crude protein; 2. Purified EgAnxB38; 3.pET32a (+) induced by IPTG; 4. EgAnxB38 incubated with rabbit anti-EgAnxB38-IgG; 5. EgAnxB38 incubated with negative rabbit serum IgG; 6. EgAnxB38 incubated with sera from a sheep infected with E. granulosus; 7. EgAnxB38 incubated with serum of healthy sheep; 8. Crude protein of PSCs incubated with rabbit anti-EgAnxB38-IgG; 9. Crude protein of PSCs incubated with negative rabbit serum IgG.

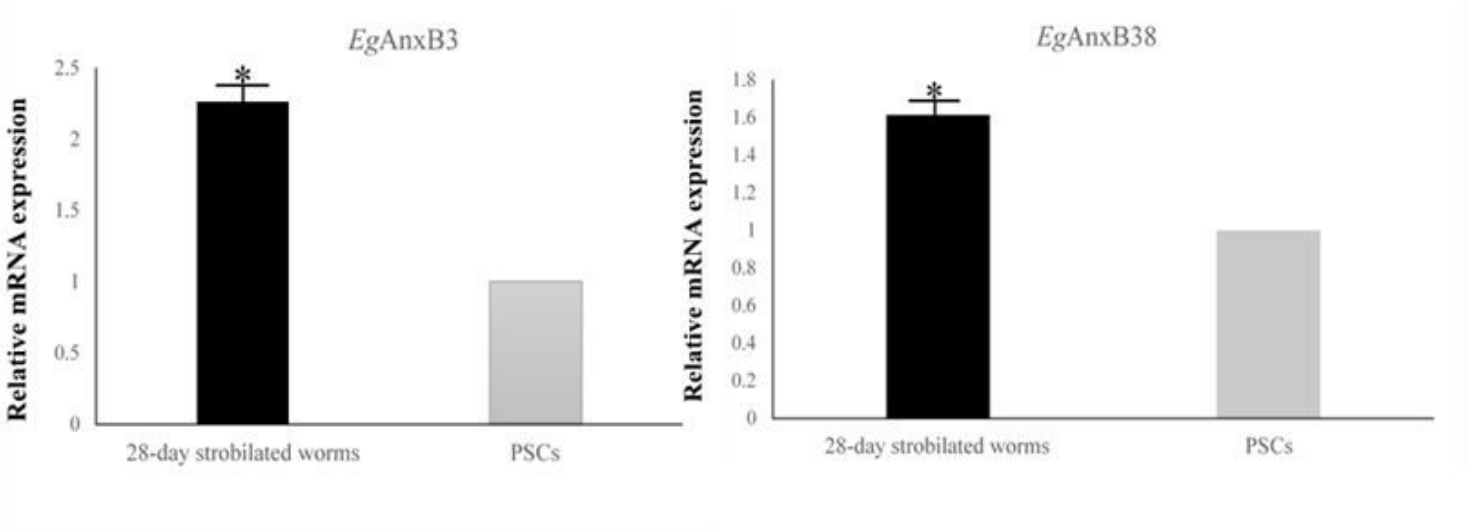

Figure 5

Comparison of transcript levels of EgAnxB3 and EgAnxB38 genes in the PSCs and adult worms (28 days). Note: Asterisks indicate statistically significant differences ($P < 0.05$) between the 28-day strobilated worms and PSCs.

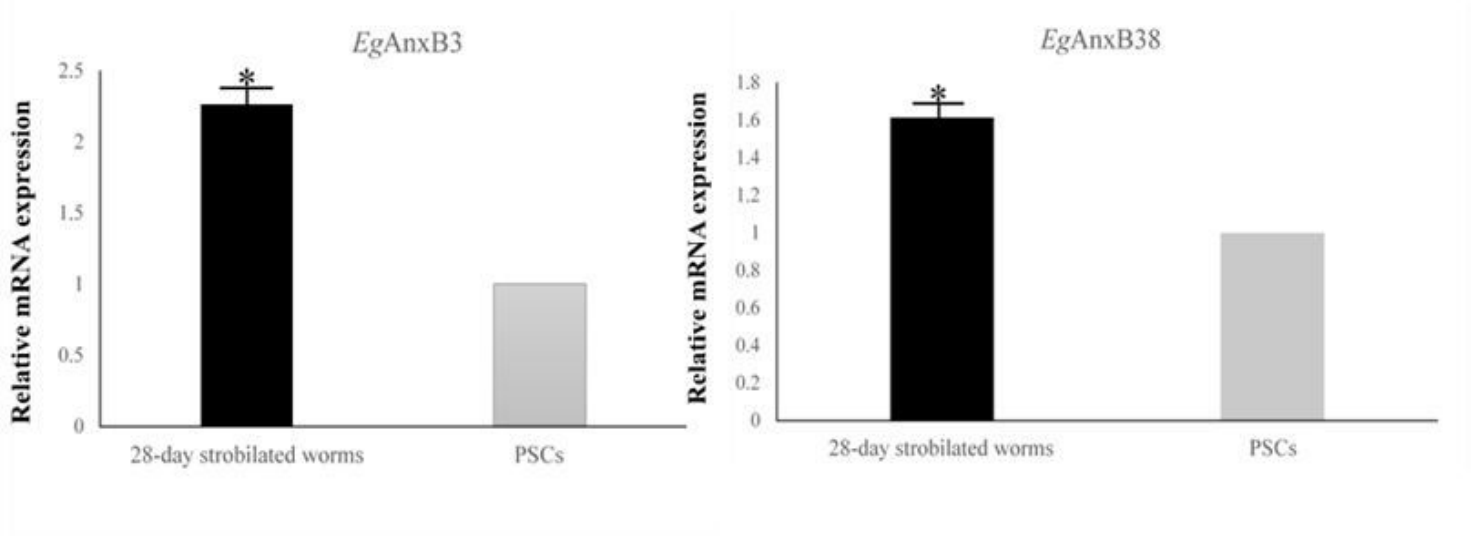

Figure 5

Comparison of transcript levels of EgAnxB3 and EgAnxB38 genes in the PSCs and adult worms (28 days). Note: Asterisks indicate statistically significant differences ($P < 0.05$) between the 28-day strobilated worms and PSCs.

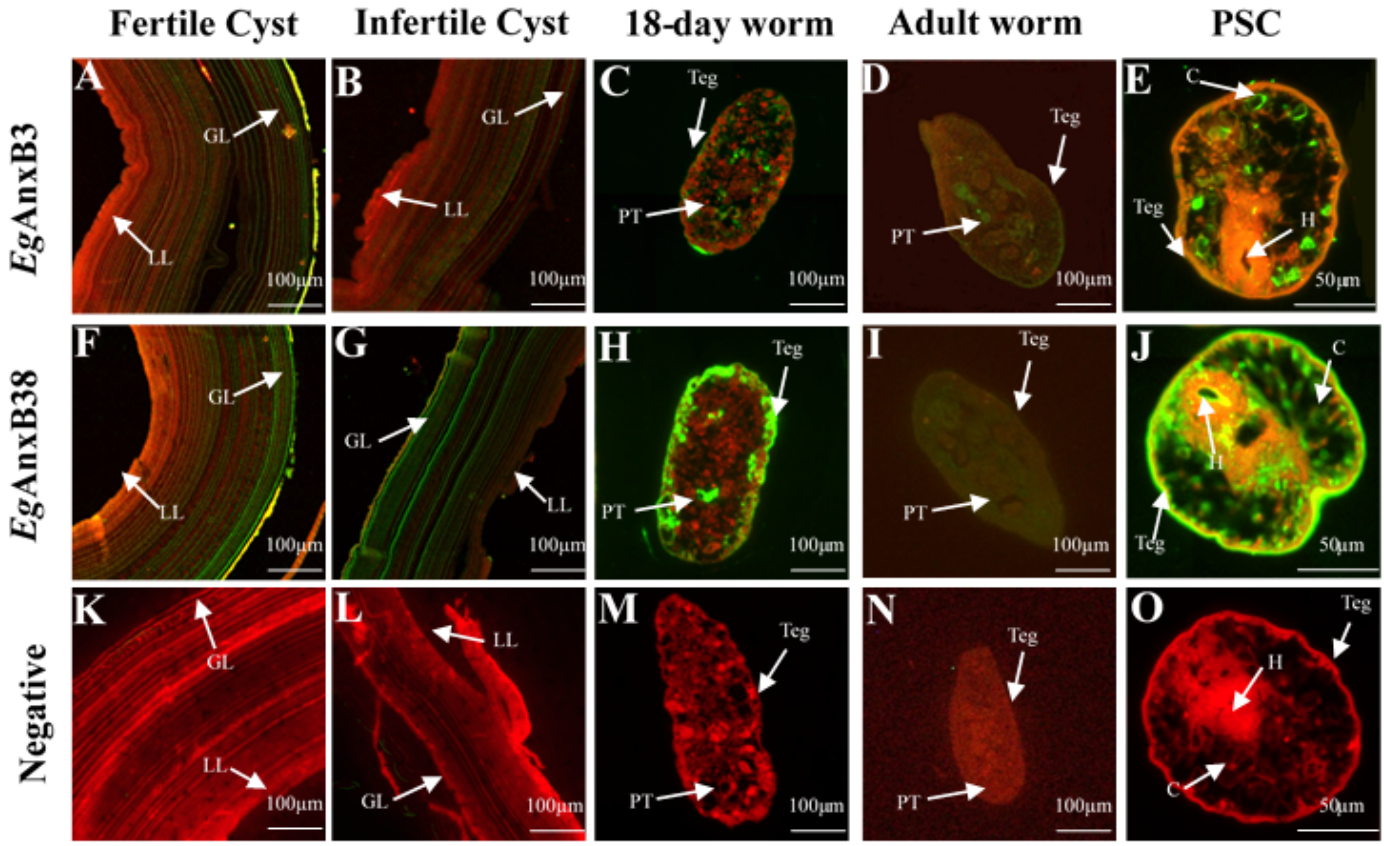

Figure 6

Immunolocalization of EgAnxB3/EgAnxB38 in different life cycle stages of E. granulosus. A–E: EgAnxB3; F–G: EgAnxB38; K–O: negative. A, F, and K: fertile cyst; B, G, and L: infertile cyst; C, H, and M: 18-day strobilated worm; D, I ,and N: 45-day adult worm; E, J, and O: PSC. The green fluorescent region is the protein distribution region. GL, germinal layer; LL, laminated layer; Teg, tegument; PT, parenchymatous tissue; H, hooks; C, calcareous corpuscles.

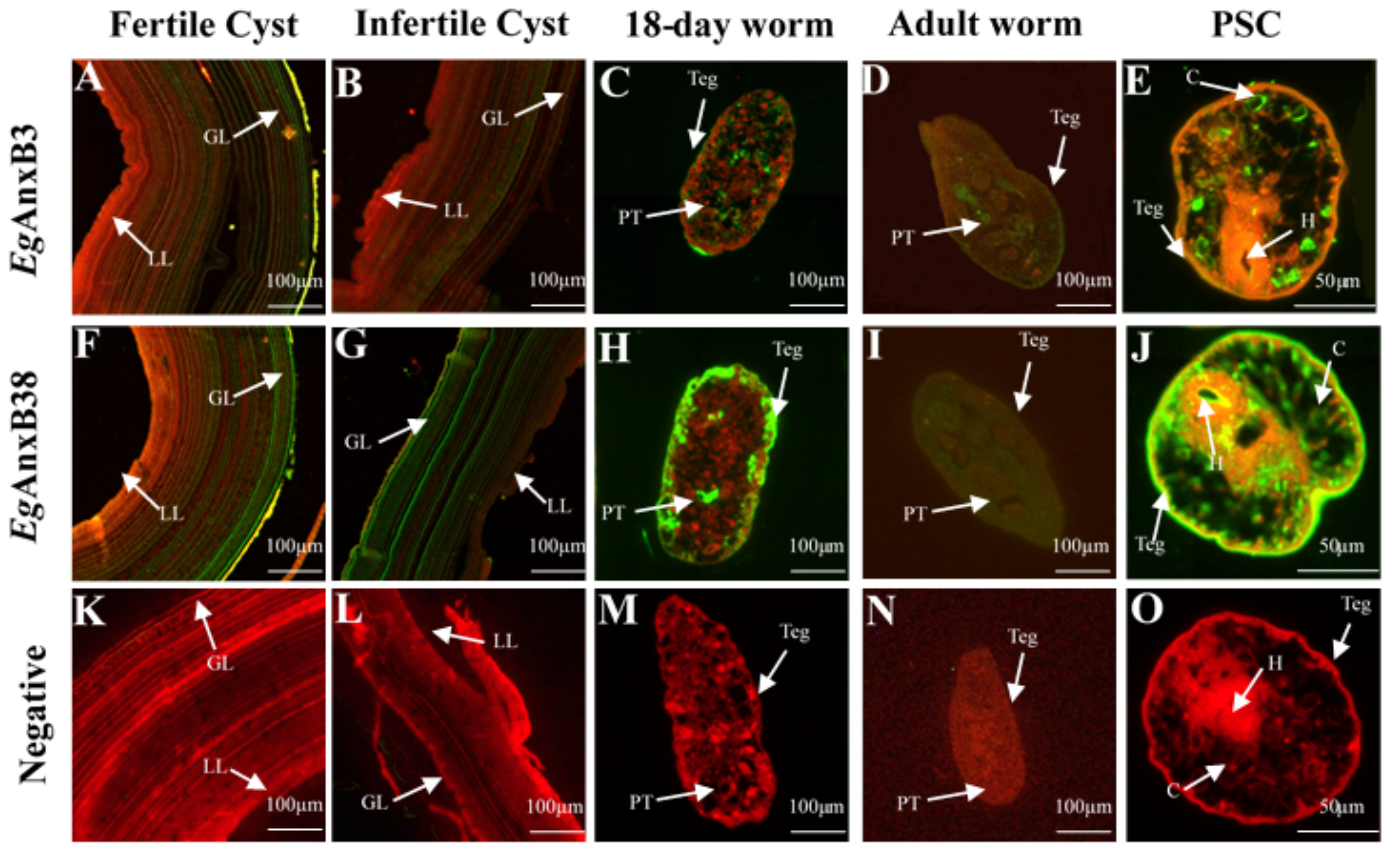

Figure 6

Immunolocalization of EgAnxB3/EgAnxB38 in different life cycle stages of E. granulosus. A–E: EgAnxB3; F–G: EgAnxB38; K–O: negative. A, F, and K: fertile cyst; B, G, and L: infertile cyst; C, H, and M: 18-day strobilated worm; D, I ,and N: 45-day adult worm; E, J, and O: PSC. The green fluorescent region is the protein distribution region. GL, germinal layer; LL, laminated layer; Teg, tegument; PT, parenchymatous tissue; H, hooks; C, calcareous corpuscles.

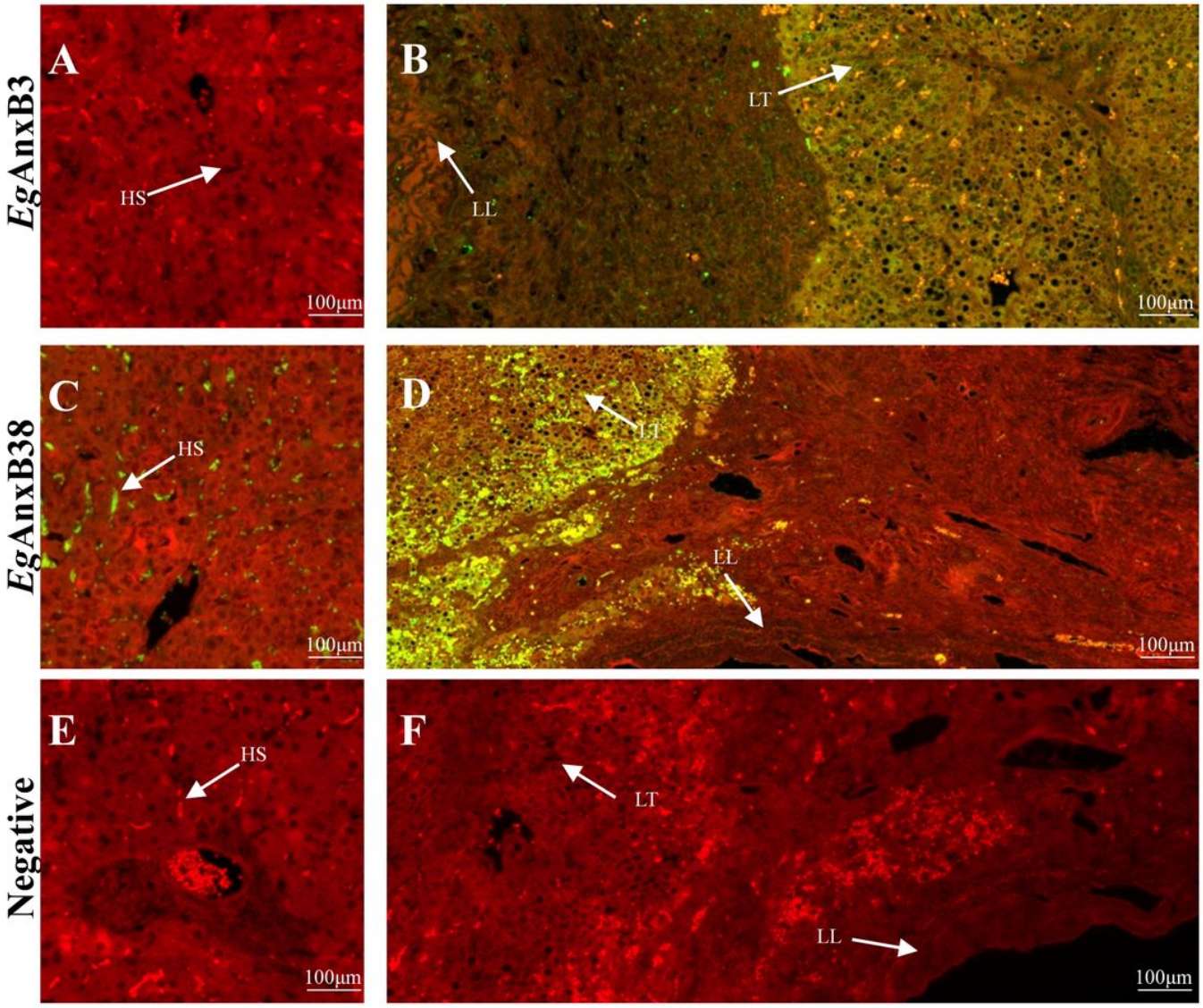

Figure 7

Immunolocalization of EgAnxB3/EgAnxB38 in different regions of sheep liver infected with E. granulosus. A and B: EgAnxB3; C and D: EgAnxB38; E and F: negative. A, C, and E: Liver tissue distant from the hydatid cysts. B, D and F: liver tissue near the hydatid cyst. The green fluorescent region is the protein distribution region. HS: hepatic sinusoid; LL, laminated layer; LT: liver tissue.

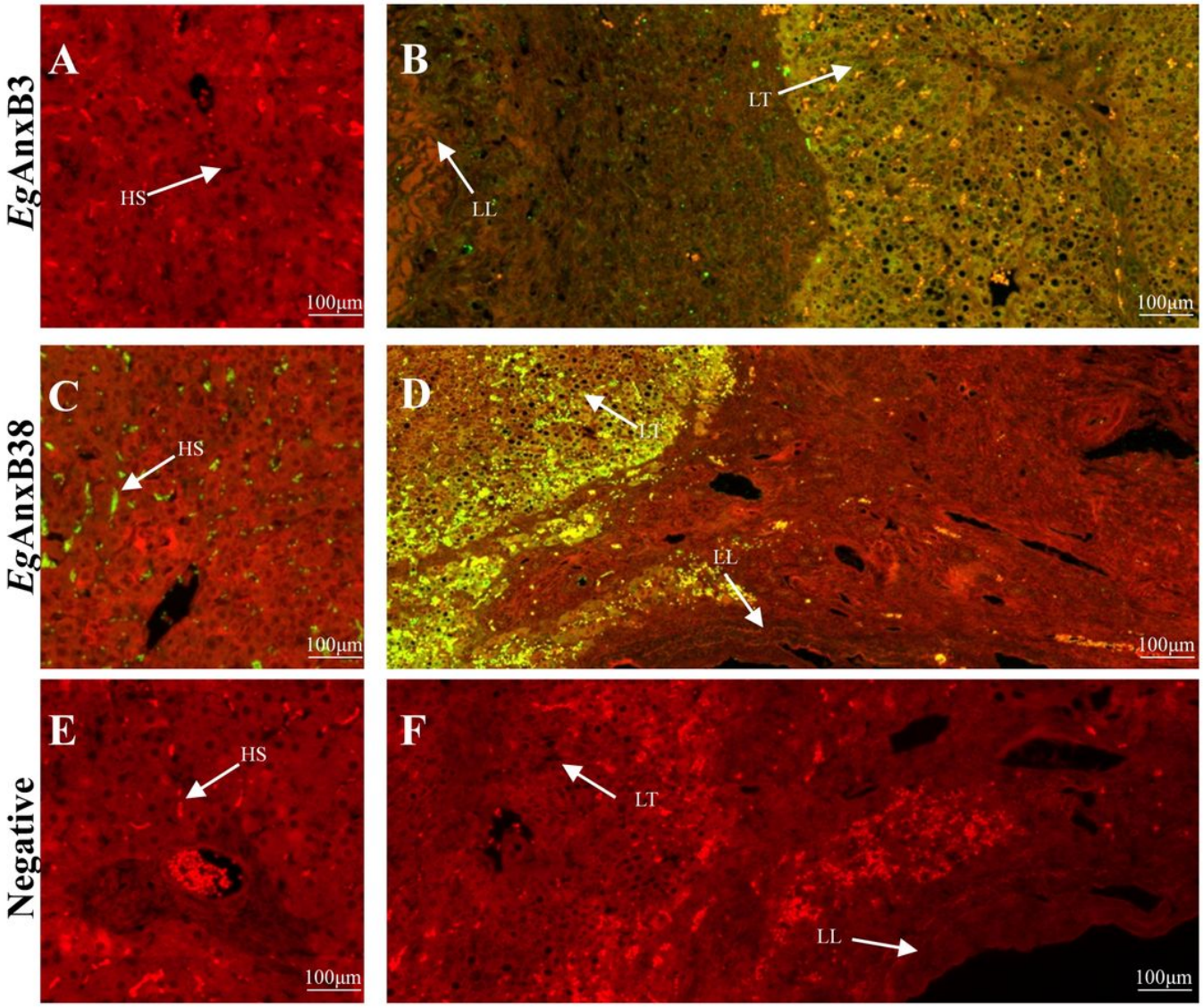

Figure 7

Immunolocalization of EgAnxB3/EgAnxB38 in different regions of sheep liver infected with E. granulosus. A and B: EgAnxB3; C and D: EgAnxB38; E and F: negative. A, C, and E: Liver tissue distant from the hydatid cysts. B, D and F: liver tissue near the hydatid cyst. The green fluorescent region is the protein distribution region. HS: hepatic sinusoid; LL, laminated layer; LT: liver tissue.

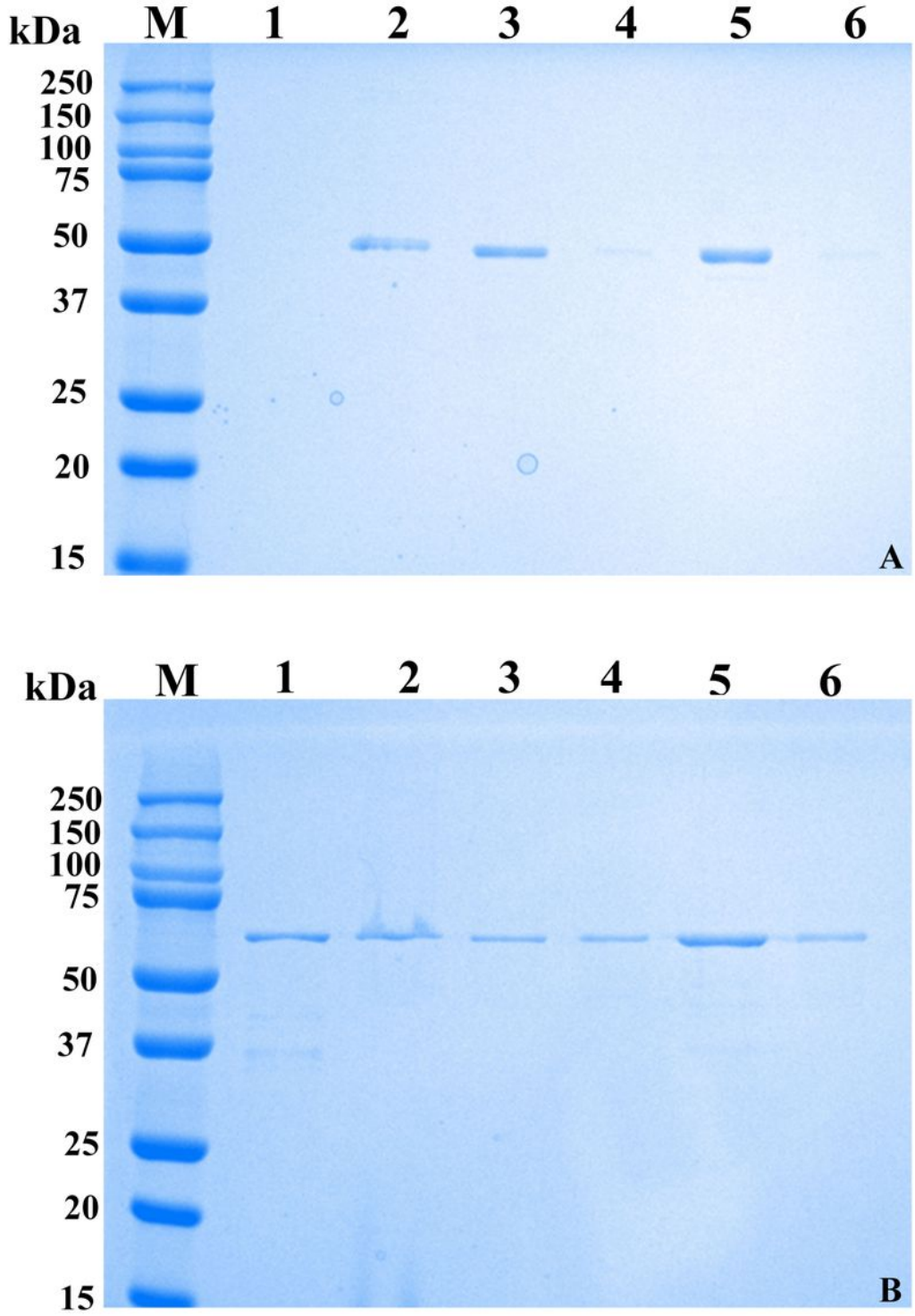

Figure 8

Phospholipid-binding properties of rEgAnxB3 and rEgAnxB38. A: EgAnxB3 B: EgAnxB38 Lane 1 and 2, rEgAnx was incubated with liposomes in buffer containing Ca2+. Lane 3 and 4, rEgAnx was incubated with liposomes in buffer containing 1 mM Ca2+ and 1 mM EDTA was then added. Lane 5 and 6, the control group (no Ca2+ or EDTA). M: Protein marker. Lane 1, 3 and 5, supernatant; lane 2, 4 and 6: precipitate.

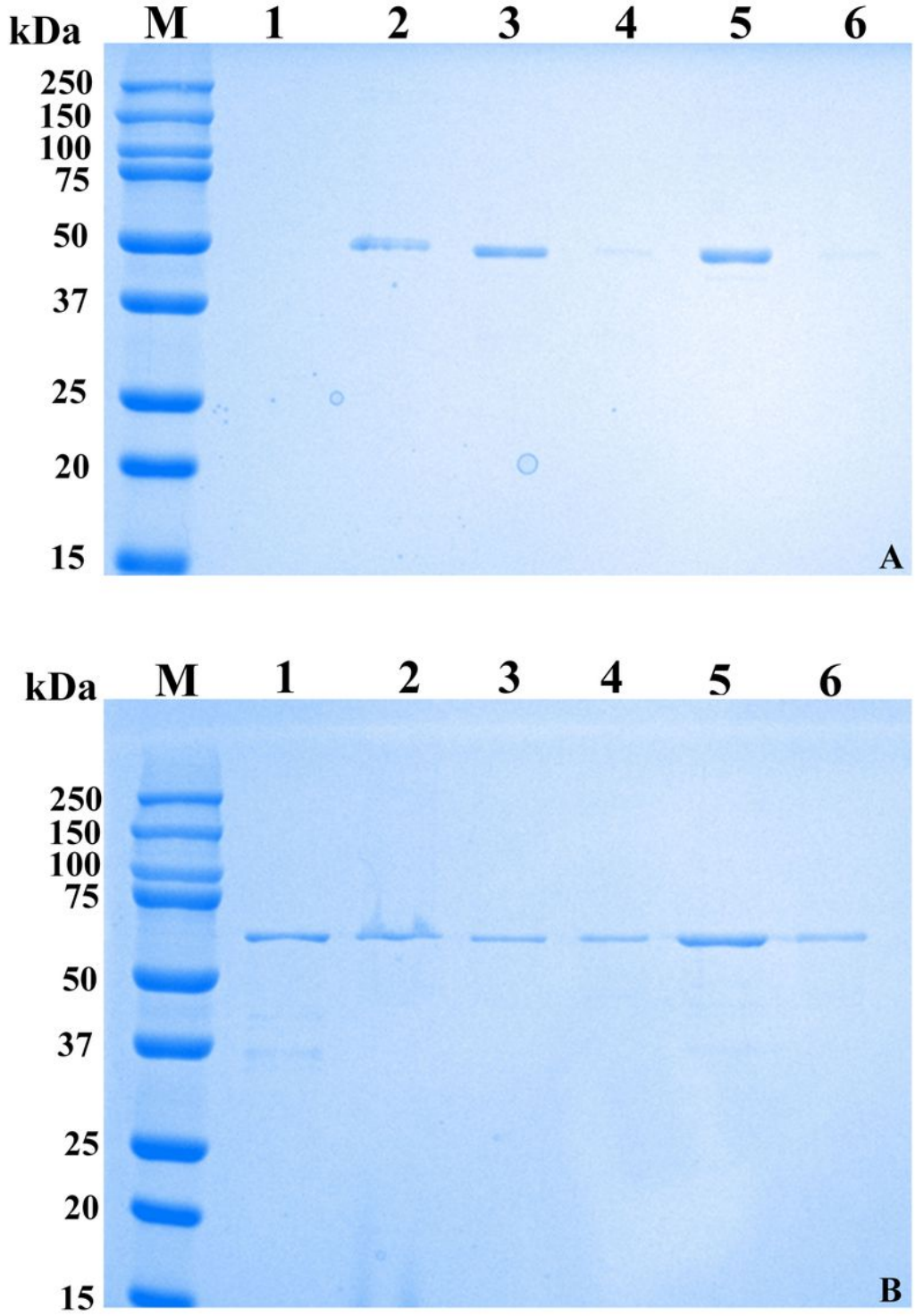

Figure 8

Phospholipid-binding properties of rEgAnxB3 and rEgAnxB38. A: EgAnxB3 B: EgAnxB38 Lane 1 and 2, rEgAnx was incubated with liposomes in buffer containing Ca2+. Lane 3 and 4, rEgAnx was incubated with liposomes in buffer containing 1 mM Ca2+ and 1 mM EDTA was then added. Lane 5 and 6, the control group (no Ca2+ or EDTA). M: Protein marker. Lane 1, 3 and 5, supernatant; lane 2, 4 and 6: precipitate.

Supplementary Files

This is a list of supplementary files associated with this preprint. Click to download.

- Graphicalabstract.png
- Graphicalabstract.png